


Article

Improving the Degradation Kinetics of Industrial Dyes with Chitosan/TiO₂/Glycerol Films for the Sustainable Recovery of Chitosan from Waste Streams

Nhung T. Tuyet Hoang ¹ and D. Duc Nguyen ^{2,3,*} 

¹ Faculty of Chemical and Food Technology, Ho Chi Minh City University of Technology and Education, 01 Vo Van Ngan Street, Thu Duc City, Ho Chi Minh City 700000, Vietnam

² Department of Environmental Energy Engineering, Kyonggi University, Suwon 16227, Republic of Korea

³ Faculty of Environmental and Food Engineering, Nguyen Tat Thanh University, 300A Nguyen Tat Thanh, District 4, Ho Chi Minh City 755414, Vietnam

* Correspondence: nguyensyduc@gmail.com

Abstract: This study investigates the potential of a combined photocatalysis–adsorption approach to effectively degrade near wash yellow (NWY), a commonly used and highly persistent dye in the textile industry, notorious for its challenging treatment and removal from wastewater due to its colorfastness. A chitosan–glycerol (CTiG) film combined with titanium dioxide was examined in both batch and continuous-flow experiments under visible solar irradiation. The results show that this combination was more effective than a pure chitosan film (60%) or chitosan–glycerol film (63%), with up to 83% degradation of NWY achieved in just 60 min of visible solar irradiation. The kinetics of the film were evaluated using both pseudo-first-order and Langmuir–Hinshelwood kinetic models. The rate constant values (k , min^{−1}) decreased with increasing NWY concentration from 20 to 80 mg/L, and k was found to be greater than twice as high under visible solar irradiation as it was in the dark. The Langmuir–Hinshelwood model's K_{LH} (reaction rate constant) and K_L (adsorption coefficient) values were 0.029 mg/L·min and 0.019 L/mg, respectively. The optimal conditions for NWY degradation were found to be 4% TiO₂ to chitosan ratio, glycerol/chitosan ratio of 40%, and a pH of 7. In the continuous-flow model, the CTiG film was submerged in an 8 L NWY solution (80 mg/L) and degraded at a rate of 22.6 mg NWY/g film under natural sunlight. This study contributes to the development of effective and sustainable methods for the degradation of dyes from textile industry wastewater.

Keywords: photocatalytic degradation; chitosan/TiO₂/glycerol films; near wash yellow dye; batch experiment; continuous-flow model



Citation: Hoang, N.T.T.; Nguyen, D.D. Improving the Degradation Kinetics of Industrial Dyes with Chitosan/TiO₂/Glycerol Films for the Sustainable Recovery of Chitosan from Waste Streams. *Sustainability* **2023**, *15*, 6979. <https://doi.org/10.3390/su15086979>

Academic Editor: Paolo S. Calabrò

Received: 4 March 2023

Revised: 17 April 2023

Accepted: 19 April 2023

Published: 21 April 2023



Copyright: © 2023 by the authors. Licensee MDPI, Basel, Switzerland. This article is an open access article distributed under the terms and conditions of the Creative Commons Attribution (CC BY) license (<https://creativecommons.org/licenses/by/4.0/>).

1. Introduction

There is increasing demand from society for colorfast textiles that maintain their original color and appearance even after multiple washings and exposure to environmental factors, such as light, heat, and chemicals [1–3]. In response to this demand, manufacturers have developed a wide range of color-resistant dyes, including azo dyes such as near wash yellow (NWY) [4]. The “near wash” characteristic of NWY dyes helps to ensure that the yellow color remains vibrant and true to shade even after multiple washings and other types of wear and tear. This helps to prolong the life of the textiles and maintain the desired appearance of the product. However, color-resistant dyes offer many benefits in terms of their performance and appearance, but they can also negatively affect the environment and human health. Some azo dyes, for example, can release harmful compounds when exposed to environmental factors, such as light, heat, or chemicals. These compounds can be toxic to aquatic life and harm the environment, and some azo dyes have also been linked to health problems in humans. Azo dyes, such as NWY dye, can be difficult to treat and remove from wastewater due to their stability and resistance to degradation [5–7].

Numerous studies have been conducted to remove toxic dyes from wastewater using physical processes (such as adsorption, filtration, and sedimentation), chemical processes (including oxidation, reduction, and neutralization), and biological and electrochemical processes [6,8–10]. Due to their durability and resistance to degradation, however, azo dyes, such as NWY, can be challenging to treat and remove from wastewater. Combination methods provide several benefits over using each method separately. Photocatalysis–adsorption is a combined approach for treating azo dyes in wastewater, in which adsorption increases the photocatalytic degradation of dyes [11,12]. In this process, azo dyes that have been destroyed by photocatalysis are extracted from wastewater using a solid adsorbent material. In addition, photocatalysis may rapidly breakdown azo dyes into less toxic compounds, while adsorption can remove the degraded colors and intermediate degradation products from wastewater, avoiding their re-entry into the environment.

Chitosan, a non-toxic, affordable, and biodegradable biopolymer, is a popular biosorbent for wastewater treatment due to its high adsorption capacity. However, dye removal using chitosan can be challenging as it requires extensive contact times, and adsorbed colors are difficult to remove [13]. To address this issue, researchers have explored the development of chitosan-based compounds that allow for phase separation following adsorption. One approach is to combine chitosan with inorganic materials, such as TiO_2 , to enhance its adsorption capabilities [14,15]. TiO_2 is a photocatalyst capable of producing reactive oxygen species (ROS) to degrade organic contaminants, incorporating TiO_2 nanopowder into chitosan to effectively regenerate the chitosan adsorbent and reduce the degradation time for dye adsorption on chitosan. The functional groups on chitosan enable the removal of colors from wastewater; the addition of TiO_2 treated the adsorbed pollutants on chitosan, and this sorbent was recovered after system operation [16]. Several studies have demonstrated the characteristics of TiO_2 /chitosan materials, their photocatalytic performance, degradation kinetics, and synergistic effects [12,17,18]. However, photocatalysis requires transparency under light irradiation; chitosan combined with TiO_2 in the form of a film facilitates the interaction of light with TiO_2 in the chitosan film. Compared to chitosan beads, the chitosan film's flat surface area allows for a larger area for light exposure, resulting in a better light absorption and higher photocatalytic activity. The drawbacks of chitosan films may not be as severe as those of other chitosan forms. In order to prevent the chitosan film from becoming brittle and breaking during the degradation process, glycerol is added as a moisturizing agent. This contributes to the preservation of the film's structural integrity and increases its durability [19]. It has been demonstrated that the combination of chitosan, TiO_2 , and glycerol is efficient at degrading colors in textile effluent. It was found that chitosan with glycerol and TiO_2 removes color more efficiently than chitosan alone; chitosan with glycerol or chitosan with TiO_2 are also effective [18].

In this study, our aim is to develop a highly efficient and sustainable method for the treatment of synthetic wastewater from the textile industry using chitosan/ TiO_2 /glycerol films fabricated using casting techniques under natural sunlight. We explored the effects of various experimental factors, such as pH, TiO_2 /chitosan ratio, glycerol/chitosan ratio, and water height, on the degradation of NWY. To evaluate the film's performance, we conducted both batch experiments with and without light irradiation to determine the pseudo-first-order and Langmuir–Hinshelwood kinetics of NWY degradation. Furthermore, we assess the film's efficacy for continuous-flow NWY degradation using a custom-designed setup. Our study provides valuable insights into the use of chitosan-based materials for wastewater treatment and their potential for the cost-effective and environmentally friendly removal of pollutants from industrial effluents.

2. Materials and Methods

2.1. Chemicals

Near Wash Yellow RCL (NearChimica, Legnano, Italy) is a high-quality dye used in the textile industry (Phong Phu Jean Company, Ho Chi Minh City, Vietnam) that is resistant to fading, washing, and sunlight (Figure 1). NWY was utilized to evaluate the

capability of films to degrade color. The films were made by combining chitosan (91.6% deacetylated from Vietnam) and TiO_2 (commercial TiO_2 Degussa P25 from Merck). This film was formulated using glycerol (Merck, 99.5%) to enhance the tensile strength of the chitosan film and the performance of chitosan and TiO_2 . To crosslink chitosan molecules, sodium triphosphate (STTP, >98% China) was used. STTP protects chitosan's amine group due to its negatively charged phosphate group, creating an electrical connection with the amine group's hydrogen [20].

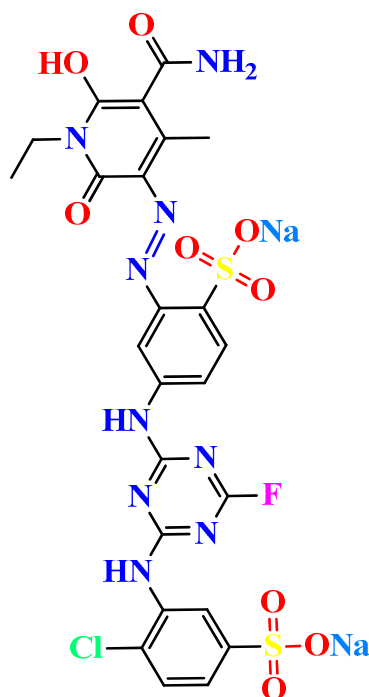


Figure 1. The molecule structure of near wash yellow [21].

2.2. Film Preparation Using Chitosan/ TiO_2 /Glycerol

A solution of 2.5% chitosan was dissolved in a solution of 5% (*v/v*) acetic acid. TiO_2 was mixed for 30 min with glycerol to produce a TiO_2 /glycerol solution. To investigate the impact of glycerol and TiO_2 on decolorization, the ratios of glycerol and TiO_2 to chitosan were 10 to 50% (*w/v*) and 1 to 6% (*w/w*), respectively. The TiO_2 /glycerol solution was, then, mixed with the chitosan solution. Within half an hour, the mixture was mixed and homogenized using a Hielscher UP 100H homogenizer. Then, the gel was poured into a (50 mm \times 100 mm \times 30 mm) glass mold and cured at 40–45 °C for 36 h. The dried films were immersed for 30 min in 1% sodium tripolyphosphate (STPP) (*w/v*) at room temperature. The wet film was then gently peeled away from the glass plate, and the residual sodium triphosphate solution was eliminated by rinsing the film with distilled water. After 8 h of drying at 70 degrees Celsius, the CTiG film was kept in a desiccator before being used for decolorization.

2.3. Photocatalytic Degradation Experiments with Near Wash Yellow Dye

2.3.1. Batch Experiment for NWY Degradation Using the Chitosan/ TiO_2 /Glycerol Film

For batch experiments on NWY degradation, 50 \times 100 mm films (pure chitosan, chitosan/glycerol, and chitosan/ TiO_2 /glycerol) were utilized (Figure 2). The films were submerged in 20 mL of NWY solution at a range of concentrations (20 to 80 mg/L). The range of pH values was between 3 and 9. The photocatalytic studies were run in the afternoon with a sunlight intensity $>30 \text{ W/m}^2$. To analyze the mechanism of photocatalysis and adsorption, the experiments were carried out for 105 min under two conditions: with and without light.

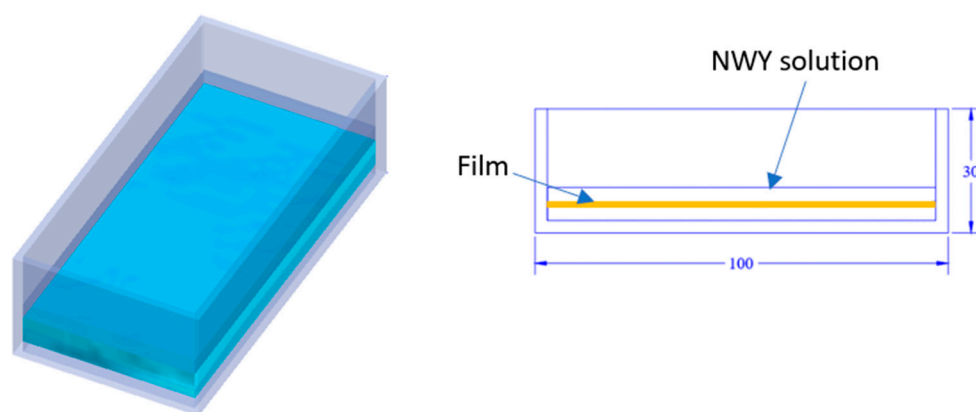


Figure 2. The batch experimental design for NWY degradation using the prepared film under sunlight irradiation.

At 15 min intervals during the reaction, the sample was removed and filtered to eliminate the solid materials. The concentration of NWY in the sample was analyzed using a UV-vis Spectrophotometer (Hitachi U2910) and a calibration curve. The dye degradation (DE%) was calculated using Formula (1):

$$DE = 100 \times (C_0 - C)/C_0 \quad (1)$$

where C_0 represents the initial NWY concentrations and C represents the NWY concentration after the irradiation time.

The surface morphology and microstructure of the CTiG film were analyzed using a scanning electron microscope (FE SEMS-4800 Hitachi, Tokyo, Japan) operating in high vacuum with a spot size of 4.0 and accelerating voltage of 4 kV energy dispersive X-ray (EDS) analyzer (XRD-D8 Advance, Bruker Co., Karlsruhe, Germany). On a BRUKER D2-212917, X-ray diffraction (XRD) was used to determine the crystallinity of the film.

2.3.2. Continuous-Flow Model for NWY Degradation using the Chitosan/TiO₂/Glycerol Film

CTiG films with dimensions of 150 × 200 mm were immersed in the NWY solution under sunlight irradiation (Figure 3). The model was fed a solution with the concentrations of NWY (80 mg/L) at a flow rate of 9.1 mL/min. Every hour, a sample of the CTiG film capacity for NWY degradation was collected.

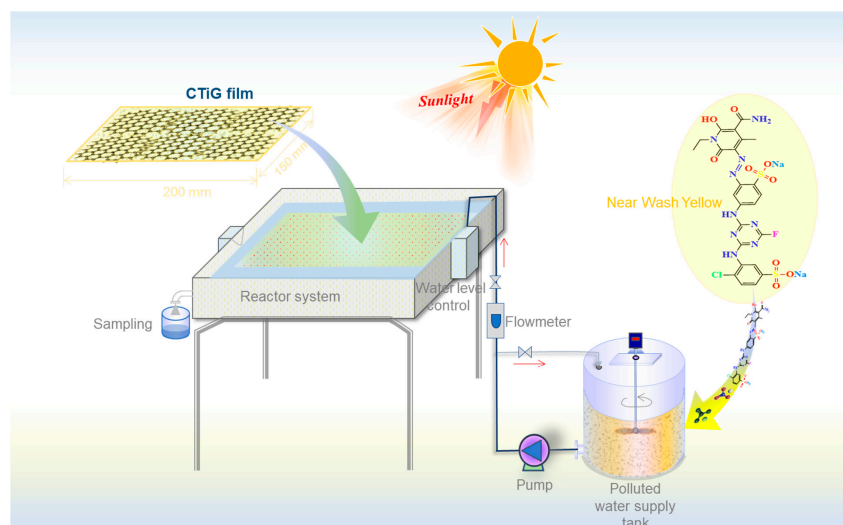


Figure 3. The continuous-flow design for NWY degradation using CTiG under sunlight irradiation.

3. Results and Discussion

3.1. CTiG Film Characterization

CTiG films had a size of 100×50 mm, thickness of 0.15 ± 0.03 mm, and density of 1.141 ± 0.12 g/cm³ (Figure 4). The chitosan film with white yellow showed no sign of opaqueness. The addition of TiO₂ nanoparticles to the chitosan solution resulted in a milky composite film, indicating a reduction in film transparency [22]. Because glycerol was used in the film-making process, the tensile strength of the CTiG film was relatively high. Glycerol increases the hydrophilicity of a film, enhancing its performance in aqueous solutions, resulting in a film that is smoother and more water-repellent.



Figure 4. Chitosan/TiO₂/glycerol film.

Combining scanning electron microscopy (SEM) with energy-dispersive X-ray spectroscopy allowed us to analyze the structure and composition of the chitosan/TiO₂ films (EDS). Based on the results of scanning electron microscopy, the distribution of TiO₂ particles on the film's surface was investigated. There were no fissures in the surface structure of the chitosan film's smooth and uniform surface (Figure 5). When TiO₂ particles on the surface of the CTiG film stuck together, tiny granules (bright spots) were formed (Figure 6).

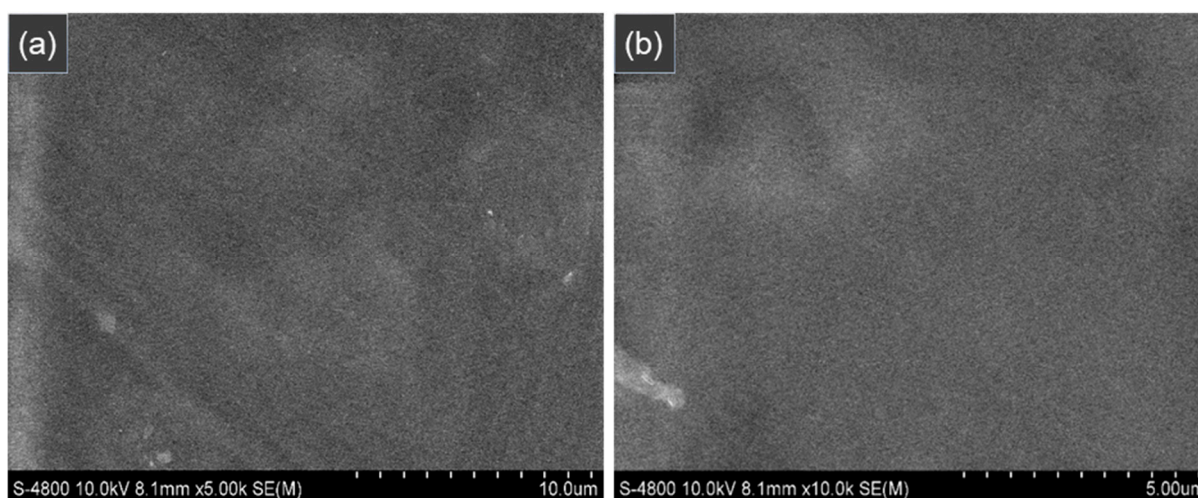


Figure 5. Scanning electron microscopy (SEM) image of the chitosan film with $\times 5000$ magnification (a) and $\times 10,000$ magnification (b).

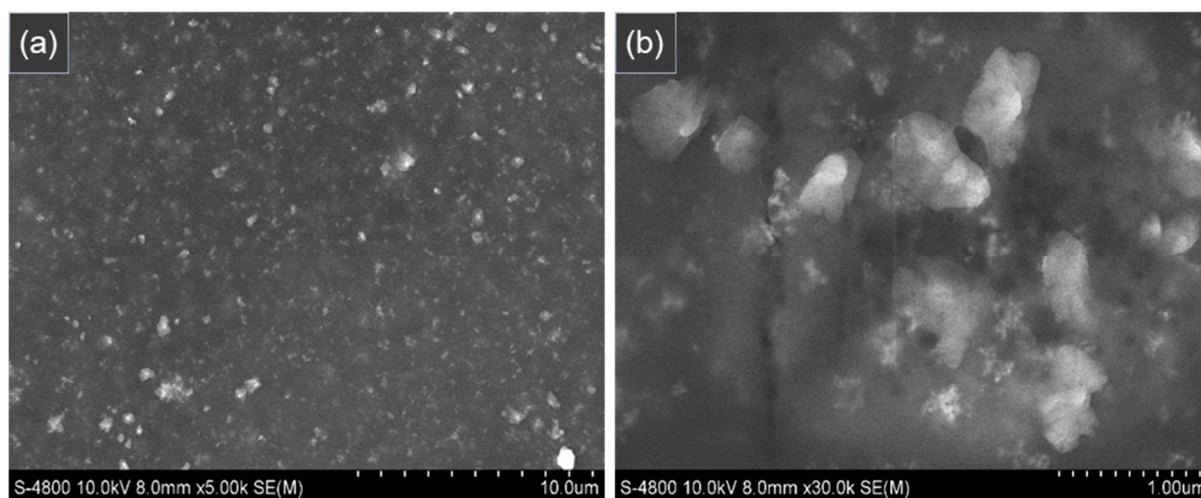


Figure 6. Scanning electron microscopy (SEM) image of the chitosan/TiO₂/glycerol (CTiG) film with $\times 5000$ magnification (a) and $\times 10,000$ magnification (b).

To verify the components of TiO₂ on the chitosan film, EDS points were carried out (Figure 7). The photos reveal that the CTiG film was composed of C, O, Ti, and P, whereas the pure chitosan film lacked Ti. Although the weight percentages of C, O, and P were not appreciably different with and without TiO₂, the relative atomic proportion of Ti ranges from 1.81 to 2.14% (Table 1). The STPP solution that crosslinks the chitosan polymer produced P [20]. The EDS analysis revealed that the nanoparticles of TiO₂ were successfully incorporated into the chitosan matrix of CTiG.

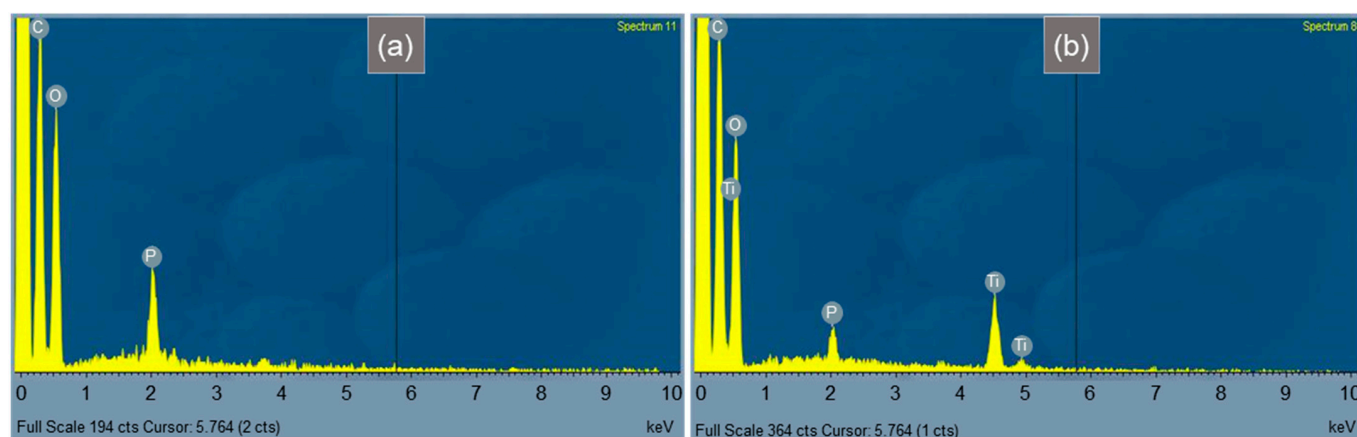


Figure 7. Energy-dispersive X-ray spectroscopy (EDS) of the chitosan (a) and chitosan/TiO₂/glycerol films (b).

Table 1. Energy-dispersive X-ray spectroscopy (EDS) results of the chitosan and chitosan/TiO₂/glycerol films.

Element	Chitosan Film	CTiG Film
C (k)	46.41–48.07	43.35–46.87
O (k)	47.33–48.68	47.09–47.26
Ti (k)	0	1.81–2.14
P (k)	4.61–4.91	3.9–7.58
Total	100.00	

Figure 8 depicts the XRD patterns of the pure chitosan, chitosan/glycerol, and chitosan/TiO₂/glycerol (CTiG) films. The diffraction of the (020) and (100) planes of the pure chitosan film were observed at 11.6 and 20.15 degrees, respectively. The (020) plane at the 11.6° peak is related to the hydrogen bonding between the chitosan and water molecules, indicating a hydrated crystalline structure. In contrast, the peak at 20.15° of the (100) plane suggests that chitosan has an amorphous structure. However, the introduction of glycerol into the pure chitosan film matrix altered its crystallographic structure. The chitosan/glycerol patterns showed a shift in the peaks of the chitosan's amorphous form to 19.9°, indicating that glycerol influenced the polymer crystallinity of the chitosan, thereby reducing its amorphous state [19]. After adding both TiO₂ and glycerol in the CTiG film, the peaks of pattern changed. Two materials may slightly decrease the amorphous state and hydrated crystalline structure of chitosan by shifting the peaks at 18.6° to 18.2° and 11.6° to 11.4°. Additionally, the diffraction of TiO₂ appeared in the CTiG film pattern at 24.9°, 37.4°, 47.6°, 53.6°, 54.7°, 62.3°, 68.7°, 69.8°, and 74.6°.

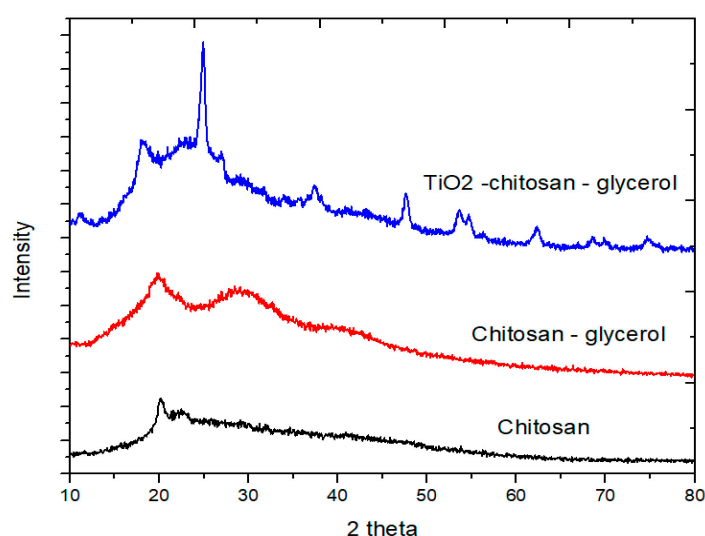
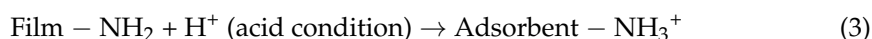
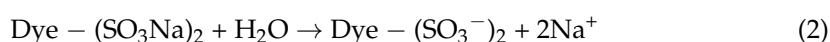


Figure 8. XRD of the pure chitosan, chitosan–glycerol, and chitosan/TiO₂/glycerol films (CTiG).

3.2. Photo-Decolorization of the CTiG Film under Natural Sunlight

3.2.1. Effect of the Reaction pH

The decolorization percentages (%) achieved with natural sunshine fell from $88.98 \pm 0.26\%$ to $75.51 \pm 0.12\%$ between pH 3 and 9, with the greatest percentages (%) obtained at pH = 3 (Figure 9). Clearly, the solution's pH plays a substantial role in the formation of hydroxyl radicals during photodegradation. In acidic conditions, chitosan molecules are sufficiently protonated by protons. This results in the production of NH_3^+ and a positive charge on the CTiG film. This positive charge is capable of attracting and absorbing negatively charged dye molecules, hence accelerating the breakdown process [23]. The acidic environment facilitates the transport of electrons from chitosan to TiO₂, resulting in the formation of electron–hole pairs. These pairs then activate oxygen species, such as hydroxyl radicals, which can breakdown organic contaminants in the solution, resulting in the elimination of color. Moreover, in acidic conditions, the dyes' sulfonic groups are negatively charged. The CTiG film might, therefore, be utilized to absorb these groups [24]. When the pH of the solution was lower than the pH_{pzc} of TiO₂ Degussa P25 (6.5) [25], the surface of the TiO₂ nanoparticles acquired a positive charge (TiOH^{2+}) [26] and attracted negative pigments more quickly.



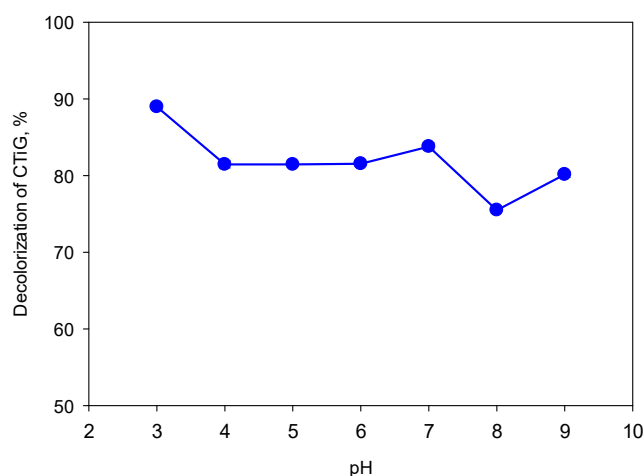
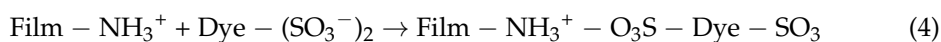


Figure 9. Effect of the pH solution on the NWY degradation of the CTiG film.

3.2.2. Effect of TiO_2 Concentration in the CTiG Film Preparation

To determine the effect of TiO_2 concentration on the decolorization of NWY, the ratio of TiO_2 to chitosan varied between 1% and 6% (*w/w*). The discoloration of NWY was depicted in Figure 10 with the dye solution at pH = 3 and pH = 7. The percentage of NWY degradation at pH values of 3 and 7 is identical. The degradation ability of the CTiG film with $\text{TiO}_2/\text{chitosan} = 1\%$ to 3% is not significantly different, ranging between 78 and 80%, and increases to $86.26 \pm 2.37\%$ (pH = 3) and $89.09 \pm 0.90\%$ when $\text{TiO}_2/\text{chitosan} = 4\%$. The higher concentration of TiO_2 nanoparticles generates more sites for the adsorption and degradation of NWY. However, the greater the ratio of TiO_2 to chitosan ($>4\%$), the lower the efficacy. TiO_2 nanoparticles may aggregate at high concentrations, reducing the number of active sites when excessive quantities of catalysts are applied. In addition, the greater the excess of catalyst, the greater the opacity of the beads, which reduces the light penetration and, consequently, the NWY degradation [27,28].

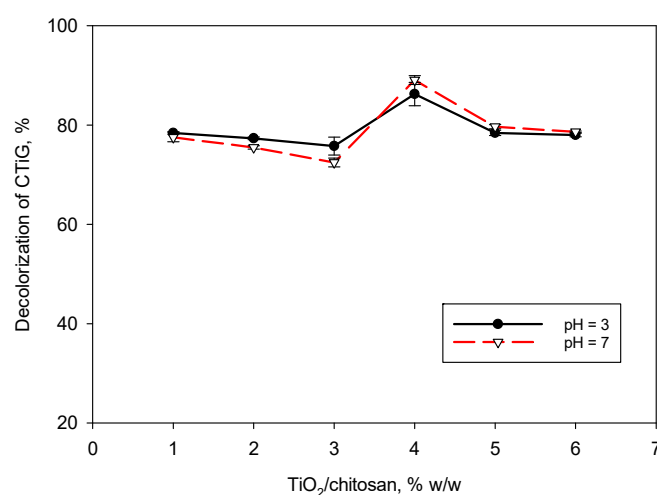


Figure 10. Effect of the percentage of TiO_2 and chitosan (*w/w*) on NWY degradation.

3.2.3. Effect of Glycerol Concentration in the CTiG Film Preparation

The influence of glycerol on the CTiG film decolorization was confirmed by increasing the glycerol/chitosan ratio in the film synthesis (Figure 11). Glycerol dramatically improves the efficiency of the film. It enhances the mechanical stability and pliability of a film, making

it more durable and manageable. Glycerol also increases the hydrophilicity of a film, hence enhancing its performance in water-based solutions [19,24]. This is because the enhanced hydrophilicity improves the interaction between the chitosan/TiO₂ layer and the pollutants in the solution, resulting in a more effective degradation process. Glycerol also enhances the dispersion of TiO₂ inside the film, resulting in a more uniform and efficient distribution of the photocatalyst. It works as an electron scavenger when coupled with TiO₂, transferring electrons to holes. In the absence of glycerol, the fast recombination of electron–hole pairs reduced the photocatalytic process. Consequently, the effectiveness of chitosan/TiO₂ in decolorizing NWY is around $61.25 \pm 2.74\%$ (pH = 3) and $58.88 \pm 0.95\%$. The introduction of glycerol leads to the creation of “glycerol clusters” that serve as hole scavengers. These clusters interact rapidly and irreversibly with the photogenerated holes, thereby increasing the life span of conduction-band electrons [29]. Thus, more free holes and electrons are formed, which can oxidize contaminants effectively [30]. The decolorization of the CTiG film increases as the glycerol/chitosan ratio rises, with the maximum level of color removal ($87.44 \pm 0.40\%$ at pH 3 and $82.45 \pm 0.38\%$ at pH 7) occurring at a glycerol/chitosan ratio of 40%. High levels of glycerol may also have a severe effect on the performance of the film. An excessive amount of glycerol can reduce the generation of reactive oxygen species (ROS) and inhibit the degradation process by interfering with the charge transfer efficiency between chitosan and TiO₂. Experiments conducted at pH 3 and pH 7 revealed that 40% was the best dose.

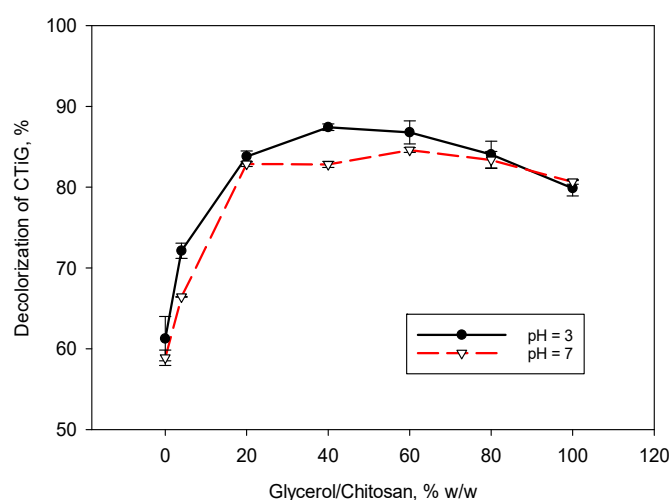


Figure 11. Effect of the percentage of glycerol and chitosan (*w/w*) on NWY degradation.

3.3. Mechanism and Kinetics of the Photo-Decolorization Using CTiG

3.3.1. Color Adsorption Using CTiG

The results of the NWY degradation under sunlight ($>30 \text{ W/m}^2$) within 105 min for the chitosan, chitosan–glycerol, and chitosan/TiO₂/glycerol films are shown on Figure 12. The effectiveness of the chitosan film after 60 min of irradiation was $57.85 \pm 0.67\%$. The chitosan–glycerol film had an efficiency of $62.1 \pm 0.60\%$, whereas chitosan–TiO₂–glycerol had an efficiency of $82.96 \pm 1.20\%$. These findings are identical to those of our previous study [18] for materials in bead form. Because of a combination of adsorption, photocatalytic oxidation, and hydrophilicity enhancement, the NWY degradation of the chitosan film combined with TiO₂ and glycerol is significantly higher than that of other films. The mechanism for the chitosan film is mostly adsorption. Chitosan has a positively charged amino group, which attracts negatively charged dyes and removes them from the solution by creating a complex. In cooperation with chitosan, glycerol can increase the hydrophilicity of the chitosan layer, hence facilitating dye adsorption [24]. In addition, glycerol can enhance the durability of the chitosan film, keeping it from degrading or dissolving over time. Therefore, the chitosan–glycerol film has a greater degradability than the chitosan film. With the addition of TiO₂ to chitosan–glycerol, the photocatalytic oxidation of NWY is

enhanced. Under UV or visible light irradiation, TiO_2 is a photocatalyst that may create reactive oxygen species (ROS), such as hydroxyl radicals ($\bullet\text{OH}$) and superoxide radicals ($\text{O}_2\bullet^-$). These ROS can oxidize the adsorbed dyes, destroying the NWY molecules and removing them from the solution. Then, chitosan can enhance adsorption following photocatalysis.

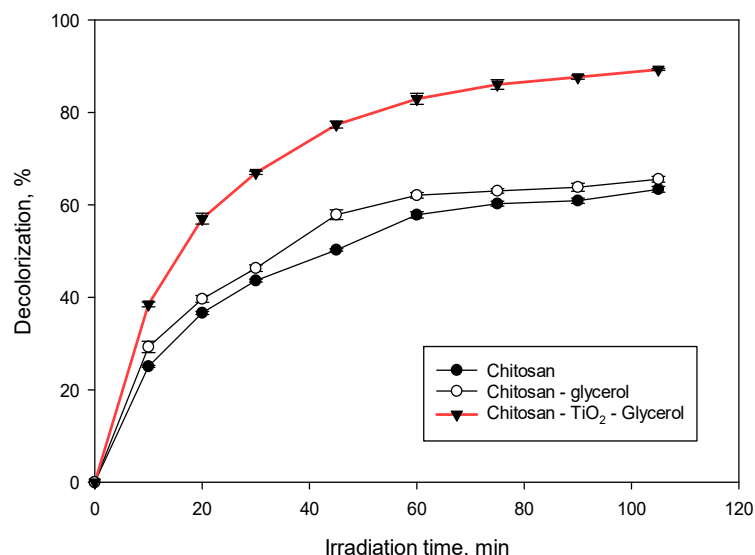


Figure 12. The NWY decolorization of the chitosan, chitosan/glycerol, and chitosan/ TiO_2 /glycerol films under sunlight irradiation.

The primary components of the CTiG film are TiO_2 and chitosan. Chitosan may absorb organic molecules, including pigments, but TiO_2 can degrade pigments when exposed to sunlight. In order to evaluate the film's capacity to decolorize owing to adsorption or photocatalysis, it is necessary to study the dye's NWY degradation process using the CTiG film with and without light. In the dark and in sunlight (UV light $> 30 \text{ W/m}^2$), the ability of CTiG to decolorize NWY at doses between 20 and 80 mg/L was evaluated (Figure 13). Clearly, the more concentrated NWY, the more efficient the decolorization. With only 60 min of irradiation, the therapy's effectiveness declined dramatically. The situation thereafter stabilized. Using a pseudo-first-order kinetic model, the kinetics of the photocatalytic CTiG degradation may be explained. The pseudo-first-order kinetic model implies that the rate of dye degradation is proportional to the difference between the initial and remaining concentrations of NWY dye [31]:

$$\ln \frac{C_0}{C} = kt \quad (5)$$

where C_0 refers to the initial NWY concentration, C is the remaining concentration of NWY, t is reaction time, and k refers to the pseudo-first-order rate constant. From the slope and intercept of these graphs, the values of rate constants were derived. As indicated in Table 2, the rate constant values k (min^{-1}) reduced with increasing the dye concentration [17]; nevertheless, the adsorption rate did not differ substantially between 40 and 80 mg/L. The estimated rate of degradation in the presence of light is twice than that in the absence of light. This reveals that the processing ability of the film under light circumstances is accelerated by photocatalysis. The study of chitosan/ TiO_2 nanomaterial for Rhodamine B and Congo red R dye had similar results [32].

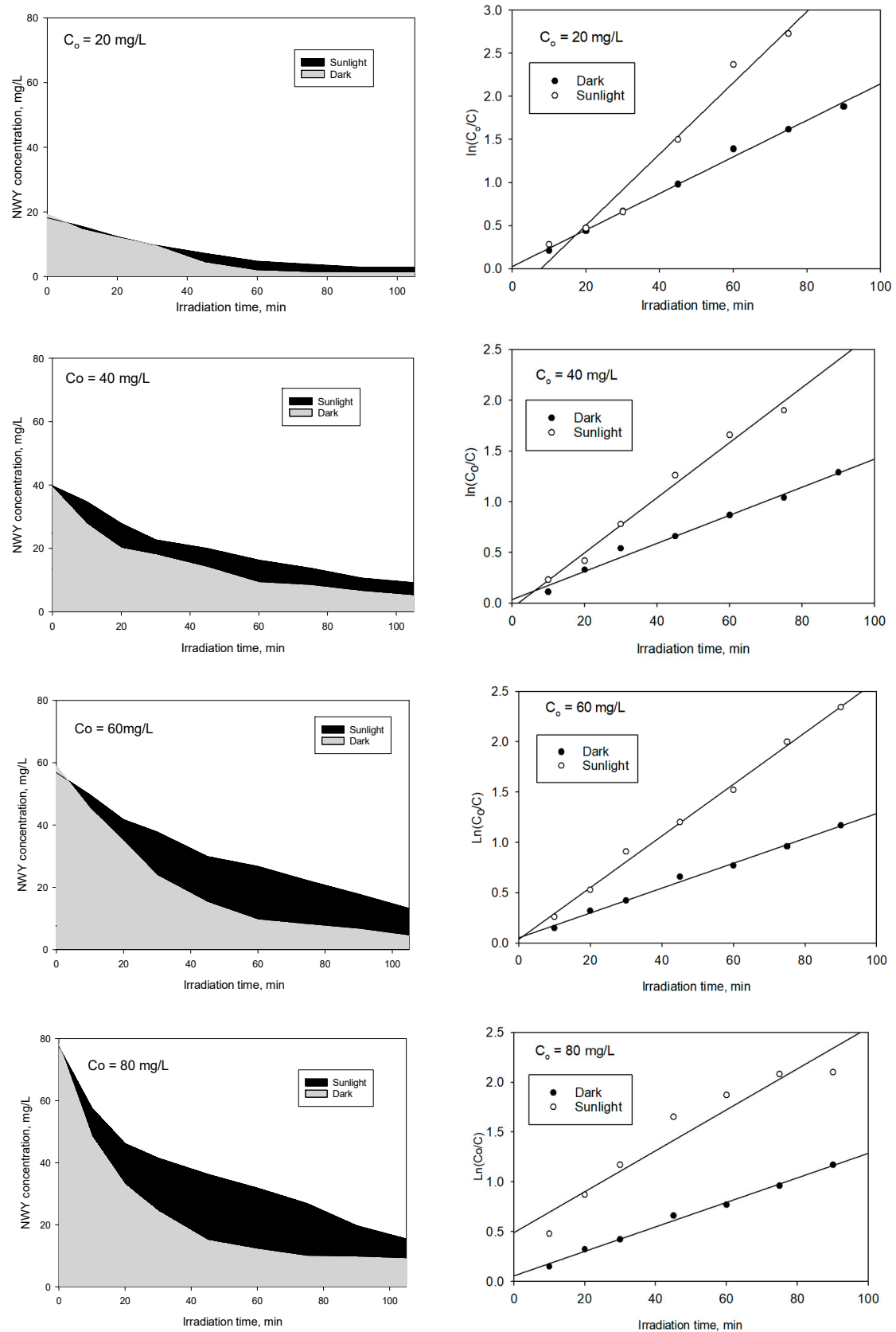


Figure 13. The pseudo-first-order kinetic model of the CTiG film for degrading NWY dye under sunlight and in darkness.

Table 2. Pseudo-first-order rate constant of the CTiG film for degrading NWY dye under sunlight and in darkness.

Co, mg/L	Dark		Sunlight	
	$k_{\text{dark}}, \text{min}^{-1}$	R^2	$k_{\text{light}}, \text{min}^{-1}$	R^2
20	0.0221	0.9958	0.0414	0.9718
40	0.0138	0.987	0.0272	0.9885
60	0.0123	0.9939	0.0256	0.9952
80	0.012	0.9765	0.0206	0.9215

3.3.2. Kinetics of the Photocatalytic Degradation

The Langmuir–Hinshelwood (L-H) model has gained popularity in recent years as a means of characterizing the kinetics of heterogeneous catalytic reactions, including photocatalytic degradation. This model establishes a relationship between the initial discoloration rate r_0 and the initial reactant concentration C_0 . To understand the dynamics of such systems, the Langmuir–Hinshelwood equation is used [33].

$$r = -\frac{dC}{dt} = \frac{k_r K_{LH}}{1 + K_{LH} C}; \quad (6)$$

where r is the rate of the reaction corresponding to the NWY concentration (C), k_r is the reaction rate coefficient (mg/L·min), and K_{LH} is the adsorption constant of the reactant material (L/mg). A linear equation may be used to obtain k_r and K_{LH} .

$$\frac{1}{r_0} = \frac{1}{k_r} + \frac{1}{k_r K_{LH} C_0}; \quad (7)$$

where r_0 is the initial degradation rate of NWY, in mg/L·min.

The linear plot of the Langmuir–Hinshelwood kinetic model is shown in Figure 14. The result proves the high linear correlation between NWY degradation and the LH kinetic model, with $R^2 = 0.9692$.

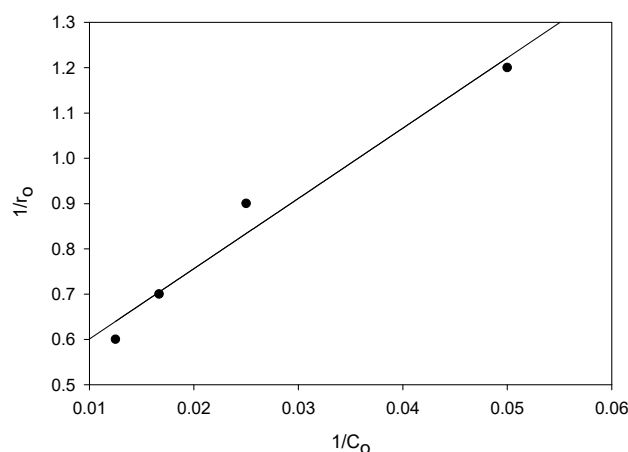
**Figure 14.** NWY degradation by CTiG represented by the Langmuir–Hinshelwood model.

Table 3 shows all the kinetic parameters calculated using the Langmuir–Hinshelwood model for NWY degradation using the CTiG film. The reaction rate constant, k_r , was calculated to be 2.241 mg/L·min, whereas the Langmuir–Hinshelwood constant, or adsorption coefficient, K_{LH} , was 0.029 L/mg.

Table 3. The pseudo-first-order and Langmuir–Hinshelwood rate constants of the CTiG film on NWY degradation under sunlight.

NWY Concentration, mg/L	Pseudo-First-Order Rate Constant, k (min^{-1})	Initial Degradation Rate Value, r_0 ($\text{mg/L} \cdot \text{min}$)	Reaction Rate Constant, k_r ($\text{mg/L} \cdot \text{min}$)	Langmuir–Hinshelwood Constant, K_{LH} (L/mg)
20	0.0414	0.828	2.241	0.029 $K_L = 0.019$
40	0.0272	1.088		
60	0.0256	1.536		
80	0.0206	1.648		

It is worth noting that there is a difference between the Langmuir–Hinshelwood adsorption constant (0.019 L/mg) in darkness and the adsorption constant under sunlight (0.029 L/mg) (Table 3). Under sunlight, the adsorption constant of the CTiG film is 1.5 times greater than that in the dark. This is because the decolorization efficiency is mostly absorbed by the chitosan coating under dark conditions, whereas the integration of the adsorption process on chitosan and the photocatalytic oxidation of titanium dioxide occurs under light conditions. Additionally, photocatalysis with TiO_2 can rapidly breakdown the molecules of the NWY dye into compounds that are less hazardous. These substances may be more readily absorbed by chitosan, resulting in the removal of damaged dyes and intermediate degradation products from wastewater, and limiting their reintroduction into the environment.

3.4. Continuous-Flow Model with the CTiG Film in NWY Degradation

3.4.1. Effect of Polluted Water Levels

Before running the continuous-flow model, water height that can influence the performance of the CTiG film in removing pollutants from a solution was reversed. The NWY degradation efficiency decreased from $86.70 \pm 0.45\%$ to $11.4 \pm 1.39\%$ when water level increased from 0.4 cm to 2 cm (Figure 15). This is owing to the fact that a shorter distance allows for a larger intensity of light to reach the film, resulting in a greater quantity of photocatalytic activity and a more effective breakdown of the pollutants [34]. A shorter distance can also increase the integrity of light dispersion on the film, resulting in a more uniform and consistent breakdown of pollutants throughout the entire film surface. However, the higher the water level, the higher the volume of polluted water, causing a greater number of contaminants to be exposed to the photocatalytic activity of the film. This is proved by experiments in which the water level increased from 0.4 to 1.4 cm (1.57 to 3.56 mg NYW/g film) during a period of 90 min. However, when water depth increases (>1.4 cm), dye degradation decreases. This might be due to the distance between the light source and the CTiG film, as well as the contamination load on the CTiG film. As a result, 1.4 cm of water level provides the best degradation performance in this case.

3.4.2. The Capacity of the CTiG Film for NWY Degradation in the Continuous-Flow Model

The continuous-flow model of the CTiG film operated in sunlight. A total of 80 mg/L of the NWY solution was pumped through the film at a flow rate of 9.1 mL/min to maintain the water level of 1.4 cm unchanged. CTiG's efficiency was around 40% at the start of model operations, similar to that of the batch experiments. The NWY load on CTiG increased as the water volume increases; hence, the efficiency of degradation reduces. After 8 L of treated water, the treatment efficacy was only 3%, and the CTiG film degraded to a maximum of 22.58 ± 0.08 mg NWY/g. After that, the NWY decrease was inconsequential (Figure 16).

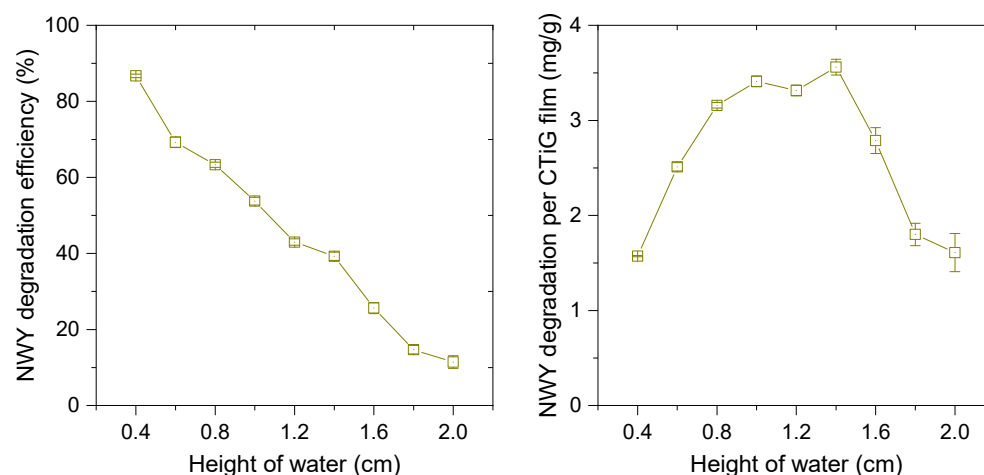


Figure 15. Effect of the water level height on the NWY degradation capacity of the GTiG film.

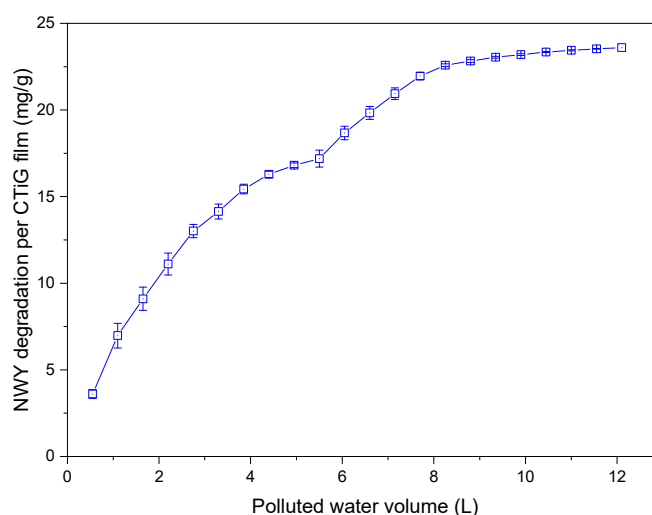


Figure 16. NWY degradation capacity of the GTiG film.

4. Conclusions

A chitosan/TiO₂/glycerol (CTiG) film was successfully fabricated using a casting method for the efficient degradation of NWY dye under natural sunlight. The integration of chitosan adsorption and TiO₂ photocatalytic oxidation in the film led to a superior NWY dye degradation compared to the pure chitosan film and the chitosan film with glycerol. Batch experiments revealed that the optimal TiO₂/chitosan and glycerol/chitosan ratios were 4% and 40%, respectively. The CTiG film was assessed using pseudo-first-order and Langmuir–Hinshelwood kinetic models under sunlight and in the dark. The predicted degradation rate constant (*k*) in the pseudo-first-order kinetic model was over twice as high under sunlight as it was in the dark. The rate constant decreased as the initial dye concentration increased from 20 to 80 mg/L. Additionally, in the continuous-flow model, operating the CTiG film at a 1.4 cm water level of NWY dye under natural sunlight resulted in 22.58 ± 0.08 mg NWY dye degradation per gram of the CTiG film. These findings demonstrate the potential of CTiG films for the sustainable recovery of chitosan from waste streams by efficiently degrading industrial dyes, such as NWY, making it a promising material for industrial wastewater treatment.

Author Contributions: Conceptualization, N.T.T.H. and D.D.N.; methodology, N.T.T.H. and D.D.N.; software, N.T.T.H.; validation, N.T.T.H.; formal analysis, N.T.T.H.; investigation, N.T.T.H. and D.D.N.; resources, N.T.T.H.; data curation, N.T.T.H.; writing—original draft preparation, N.T.T.H.; writing—review and editing, D.D.N.; supervision, N.T.T.H. and D.D.N.; project administration, N.T.T.H. and

D.D.N.; funding acquisition N.T.T.H. and D.D.N. All authors have read and agreed to the published version of the manuscript.

Funding: This research was funded by Ho Chi Minh City University of Technology and Education grant number T2022-126.

Institutional Review Board Statement: Not applicable.

Informed Consent Statement: Not applicable.

Data Availability Statement: Data can be provided upon request.

Acknowledgments: The authors would like to thank Ho Chi Minh City University of Technology and Education for providing financial assistance for the study (T2022-126).

Conflicts of Interest: The authors declare no conflict of interest.

References

1. Sahreen, S.; Mukhtar, H. Development of Bacterial Augmented Floating Treatment Wetlands System (FTWs) for Eco-Friendly Degradation of Malachite Green Dye in Water. *Sustainability* **2023**, *15*, 4541. [\[CrossRef\]](#)
2. Jahan, N.; Tahmid, M.; Shoronika, A.Z.; Fariha, A.; Roy, H.; Pervez, M.N.; Cai, Y.; Naddeo, V.; Islam, M.S. A Comprehensive Review on the Sustainable Treatment of Textile Wastewater: Zero Liquid Discharge and Resource Recovery Perspectives. *Sustainability* **2022**, *14*, 15398. [\[CrossRef\]](#)
3. Furferi, R.; Volpe, Y.; Mantellassi, F. Circular Economy Guidelines for the Textile Industry. *Sustainability* **2022**, *14*, 11111. [\[CrossRef\]](#)
4. Yaseen, D.A.; Scholz, M. Textile dye wastewater characteristics and constituents of synthetic effluents: A critical review. *Int. J. Environ. Sci. Technol.* **2018**, *16*, 1193–1226. [\[CrossRef\]](#)
5. Yaseen, Z.M.; Zigale, T.T.; Tiyyasha, D., R.K.; Salih, S.Q.; Awasthi, S.; Tung, T.M.; Al-Ansari, N.; Bhagat, S.K. Laundry wastewater treatment using a combination of sand filter, bio-char and teff straw media. *Sci. Rep.* **2019**, *9*, 18709. [\[CrossRef\]](#)
6. López-Casaperalta, P.; Molina-Rodríguez, F.N.; Fernandez-F, F.; Díaz-Quintanilla, J.F.; Barreda-Del-Carpio, J.E.; Bernabe-Ortiz, J.C.; Aguilar-Pineda, J.A. Optimization of a Textile Effluent Treatment System and Evaluation of the Feasibility to Be Reused as Influent in Textile Dyeing Processes. *Sustainability* **2022**, *14*, 15588. [\[CrossRef\]](#)
7. Lara, L.; Cabral, I.; Cunha, J. Ecological Approaches to Textile Dyeing: A Review. *Sustainability* **2022**, *14*, 8353. [\[CrossRef\]](#)
8. Matoh, L.; Žener, B.; Genorio, B. Green Synthesis of Immobilized CuO Photocatalyst for Disinfection of Water. *Sustainability* **2022**, *14*, 10581. [\[CrossRef\]](#)
9. Villabona-Ortiz, Á.; Figueroa-Lopez, K.J.; Ortega-Toro, R. Kinetics and Adsorption Equilibrium in the Removal of Azo-Anionic Dyes by Modified Cellulose. *Sustainability* **2022**, *14*, 3640. [\[CrossRef\]](#)
10. Luo, X.; Liang, C.; Hu, Y. Comparison of Different Enhanced Coagulation Methods for Azo Dye Removal from Wastewater. *Sustainability* **2019**, *11*, 4760. [\[CrossRef\]](#)
11. Ajiboye, T.O.; Oyewo, O.A.; Onwudiwe, D.C. Adsorption and photocatalytic removal of Rhodamine B from wastewater using carbon-based materials. *Flatchem* **2021**, *29*, 100277. [\[CrossRef\]](#)
12. Jimenez-Relinque, E.; Lee, S.F.; Plaza, L.; Castellote, M. Synergetic adsorption–photocatalysis process for water treatment using TiO₂ supported on waste stainless steel slag. *Environ. Sci. Pollut. Res.* **2022**, *29*, 39712–39722. [\[CrossRef\]](#) [\[PubMed\]](#)
13. Grzybnek, P.; Jakubski, Ł.; Dudek, G. Neat Chitosan Porous Materials: A Review of Preparation, Structure Characterization and Application. *Int. J. Mol. Sci.* **2022**, *23*, 9932. [\[CrossRef\]](#) [\[PubMed\]](#)
14. Pal, P.; Pal, A. Dye removal using waste beads: Efficient utilization of surface-modified chitosan beads generated after lead adsorption process. *J. Water Process Eng.* **2019**, *31*, 100882. [\[CrossRef\]](#)
15. Rasoulifard, M.H.; Seyed Dorraji, M.S.; Mozafari, V. Visible light photocatalytic activity of chitosan/poly(vinyl alcohol)/TiO₂ nanocomposite for dye removal: Taguchi-based optimization. *Environ. Prog. Sustain. Energy* **2017**, *36*, 66–72. [\[CrossRef\]](#)
16. Bahrudin, N.N.; Nawli, M.A. Mechanistic of photocatalytic decolorization and mineralization of methyl orange dye by immobilized TiO₂/chitosan-montmorillonite. *J. Water Process Eng.* **2019**, *31*, 100843. [\[CrossRef\]](#)
17. Farzana, M.H.; Meenakshi, S. Synergistic Effect of Chitosan and Titanium Dioxide on the Removal of Toxic Dyes by the Photodegradation Technique. *Ind. Eng. Chem. Res.* **2013**, *53*, 55–63. [\[CrossRef\]](#)
18. Hoang, N.T.-T.; Tran, A.T.-K.; Hoang, M.-H.; Nguyen, T.T.H.; Bui, X.-T. Synergistic effect of TiO₂/chitosan/glycerol photocatalyst on color and COD removal from a dyeing and textile secondary effluent. *Environ. Technol. Innov.* **2021**, *21*, 101255. [\[CrossRef\]](#)
19. Kusmono; Wildan, M.W.; Lubis, F.I. Fabrication and Characterization of Chitosan/Cellulose Nanocrystal/Glycerol Bio-Composite Films. *Polymers* **2021**, *13*, 1096. [\[CrossRef\]](#)
20. L. Dantas, M.J.; F. dos Santos, B.F.; A. Tavares, A.; Maciel, M.A.; Lucena, B.d.M.; L. Fook, M.V.; de L. Silva, S.M. The Impact of the Ionic Cross-Linking Mode on the Physical and in Vitro Dexamethasone Release Properties of Chitosan/Hydroxyapatite Beads. *Molecules* **2019**, *24*, 4510. [\[CrossRef\]](#)
21. Tran, A.T.-K.; Hoang, N.T.-T.; Hoang Nguyen, T.T. Combination of photocatalytic degradation and adsorption in dye removal by TiO₂-chitosan-glycerol beads under natural sunlight. *IOP Conf. Ser. Earth Environ. Sci.* **2022**, *964*, 012028. [\[CrossRef\]](#)

22. Taspika, M.; Desiati, R.D.; Mahardika, M.; Sugiarti, E.; Abral, H. Influence of TiO₂/Ag particles on the properties of chitosan film. *Adv. Nat. Sci. Nanosci. Nanotechnol.* **2020**, *11*, 015017. [[CrossRef](#)]
23. Yoshida, H.; Okamoto, A.; Kataoka, T. Adsorption of acid dye on cross-linked chitosan fibers: Equilibria. *Chem. Eng. Sci.* **1993**, *48*, 2267–2272. [[CrossRef](#)]
24. Basiak, E.; Lenart, A.; Debeaufort, F. How Glycerol and Water Contents Affect the Structural and Functional Properties of Starch-Based Edible Films. *Polymers* **2018**, *10*, 412. [[CrossRef](#)] [[PubMed](#)]
25. Hu, C.; Yu, J.C.; Hao, Z.; Wong, P.K. Effects of acidity and inorganic ions on the photocatalytic degradation of different azo dyes. *Appl. Catal. B Environ.* **2003**, *46*, 35–47. [[CrossRef](#)]
26. Fox, M.A.; Dulay, M.T. Heterogeneous photocatalysis. *Chem. Rev.* **1993**, *93*, 341–357. [[CrossRef](#)]
27. Mortazavian, S.; Saber, A.; James, D.E. Optimization of Photocatalytic Degradation of Acid Blue 113 and Acid Red 88 Textile Dyes in a UV-C/TiO₂ Suspension System: Application of Response Surface Methodology (RSM). *Catalysts* **2019**, *9*, 360. [[CrossRef](#)]
28. Sohrabi, M.R.; Ghavami, M. Photocatalytic degradation of Direct Red 23 dye using UV/TiO₂: Effect of operational parameters. *J. Hazard. Mater.* **2008**, *153*, 1235–1239. [[CrossRef](#)]
29. Panagiotopoulou, P.; Karamerou, E.E.; Kondarides, D.I. Kinetics and mechanism of glycerol photo-oxidation and photo-reforming reactions in aqueous TiO₂ and Pt/TiO₂ suspensions. *Catal. Today* **2013**, *209*, 91–98. [[CrossRef](#)]
30. Pitcher, M.W.; Emin, S.M.; Valant, M. A Simple Demonstration of Photocatalysis Using Sunlight. *J. Chem. Educ.* **2012**, *89*, 1439–1441. [[CrossRef](#)]
31. Sabarudin, A.; Madjid, A.D.R. Preparation and Kinetic Studies of Cross-Linked Chitosan Beads Using Dual Crosslinkers of Tripolyphosphate and Epichlorohydrin for Adsorption of Methyl Orange. *Sci. World J.* **2021**, *2021*, 6648457. [[CrossRef](#)] [[PubMed](#)]
32. Karthikeyan, K.T.; Nithya, A.; Jothivenkatachalam, K. Photocatalytic and antimicrobial activities of chitosan-TiO₂ nanocomposite. *Int. J. Biol. Macromol.* **2017**, *104*, 1762–1773. [[CrossRef](#)] [[PubMed](#)]
33. Kumar, K.V.; Porkodi, K.; Rocha, F. Langmuir–Hinshelwood kinetics—A theoretical study. *Catal. Commun.* **2008**, *9*, 82–84. [[CrossRef](#)]
34. Heredia Deba, S.A.; Wols, B.A.; Yntema, D.R.; Lammertink, R.G.H. Photocatalytic ceramic membrane: Effect of the illumination intensity and distribution. *J. Photochem. Photobiol. A Chem.* **2023**, *437*, 114469. [[CrossRef](#)]

Disclaimer/Publisher’s Note: The statements, opinions and data contained in all publications are solely those of the individual author(s) and contributor(s) and not of MDPI and/or the editor(s). MDPI and/or the editor(s) disclaim responsibility for any injury to people or property resulting from any ideas, methods, instructions or products referred to in the content.